Structural and Viscoelastic Properties of Actin/Filamin Networks: Cross-Linked versus Bundled Networks

K. M. Schmoller,[†] O. Lieleg,[†‡] and A. R. Bausch[†*]
[†]Lehrstuhl für Zellbiophysik E27, Technische Universität München, Garching, Germany; and [‡]Faculty of Arts and Sciences, Center for Systems Biology, Harvard University, Cambridge, Massachusetts

ABSTRACT The high diversity of cytoskeletal actin structures is accomplished by myriads of actin binding proteins (ABPs). Depending on its concentration, even a single type of ABP can induce different actin microstructures. Thus, for an overall understanding of the cytoskeleton, a detailed characterization of the cross-linker's effect on structural and mechanical properties of actin networks is required for each ABP. Using confocal microscopy and macrorheology, we investigate both cross-linked and bundled actin/filamin networks and compare their microstructures as well as their viscoelastic properties in the linear and the nonlinear regime.

INTRODUCTION

Actin is a major component of the cytoskeleton, which accounts for the mechanical stability as well as motility of cells (1,2). The numerous tasks of the cytoskeleton are achieved by a huge variety of actin binding proteins (ABPs), which accomplish a precisely tailored arrangement of actin filaments. The locally differing microstructures are built and maintained by cross-linking molecules, which are a major class of ABPs. Their effect on the mechanical properties of actin networks has been studied extensively over the past years by both reconstituting and simulating in vitro model systems with varying degrees of complexity (3–10). It has turned out that the high complexity of the cytoskeleton is reflected by the fact that each cross-linking molecule has its own characteristic effect on the structural and mechanical network properties (3,11–16). Until now, it was widely believed that such reconstituted actin networks should be well equilibrated. However, recent results show that this is not necessarily the case: Actin/α-actinin and actin/filamin bundle networks have been shown to be kinetically trapped (17,18). Moreover, actin/filamin networks exhibit significant internal stresses. Filamins are ABPs, which fulfill multiple tasks: They cross-link and bundle actin filaments but also play an important role as signaling proteins in vivo (19,20). Actin networks cross-linked by filamin have been shown to exhibit a drastic macroscopic stress hardening behavior: By applying a prestress, the nonlinear stiffness can be tuned over several orders of magnitude while the linear network elasticity remains moderate (21). This is in contrast to, e.g., cross-linked actin/heavy meromyosin (HMM) networks, where addition of HMM results in a very strong increase of the linear network elasticity (22). In the case of filamentous actin/filamin networks, the nonlinear behavior can be attributed to the high flexibility of the individual filamin molecules (21,23). On the other hand, in actin/filamin bundle networks, the branched and merged network microstructure (12) might as well be responsible for the remarkable nonlinear viscoelastic behavior of the network.

The complex microstructure of such branched bundle networks may be the result of an aggregation controlled growth process, which is also responsible for the aster formation in networks cross-linked by α-actinin (17). A further complication arises from the fact that the formation of distinct microstructures depends not only on the molar ratio between a cross-linking ABP and actin, $R_{ABP} = c_{ABP}/c_a$, but also on the actin concentration c_a itself (24). Thus, especially for such systems showing structural polymorphism, a thorough investigation of the viscoelastic network response and its correlation with the various microstructures is needed before suitable theoretical models can be developed and tested.

Here, we present a detailed characterization of the structural and macromechanical properties of actin/filamin networks. Depending on the actin and filamin concentrations, two distinct regimes can be distinguished. Within the first concentration regime, filamin not only cross-links actin filaments, but also changes the network structure by inducing the formation of bundles, which results in an enhancement of the linear as well as the nonlinear network stiffness. At high filamin concentrations, purely bundled networks emerge, which contain bundle clusters at high actin concentrations. In the bundle regime, we observe a structural saturation, which is accompanied by an insensitivity of nonlinear viscoelastic network properties with respect to the filamin concentration.

MATERIALS AND METHODS

G-actin is obtained from rabbit skeletal muscle and stored in lyophilized form at −21°C (25). The G-actin solution is prepared by dissolving lyophilized actin in deionized water and dialyzing against G-buffer (2 mM Tris, 0.2 mM ATP, 0.2 mM $CaCl_2$, 0.2 mM DTT, and 0.005% NaN_3, pH 8) at

Submitted December 2, 2008, and accepted for publication April 22, 2009.

*Correspondence: abausch@ph.tum.de

Editor: Marileen Dogterom.

© 2009 by the Biophysical Society

0006-3495/09/07/0083/7 $2.00

doi: 10.1016/j.bpj.2009.04.040

4°C. The G-actin solution is kept at 4°C and used within 10 days. The average length of the actin filaments is controlled to 21 μm by adjusting the molar ratio between actin and gelsolin (26) obtained from bovine plasma serum following Kurokawa et al. (27). Representative regions of the phase space have also been tested without gelsolin, but no significant change in the structural state diagram (see Fig. 3) has been observed (data not shown). Muscle filamin was isolated from chicken gizzard and further purified as reported in Shizuta et al. (28). The viscoelastic response of actin/ABP-networks is determined by measuring the frequency-dependent viscoelastic moduli $G'(f)$ and $G''(f)$ with a stress-controlled rheometer (Physica MCR 301; Anton Paar, Graz, Austria) over a frequency range of three decades. Polymerization is initiated by adding 10% volume 10× F-buffer (20 mM Tris, 5 mM ATP, 20 mM $MgCl_2$, 2 mM $CaCl_2$, 1 M KCl, and 2 mM DTT, pH 7.5). Approximately 480 μL sample volume is loaded within 1 min into the rheometer using a 50-mm plate-plate geometry with 160-μm plate separation. Actin polymerization is carried out in situ, and measurements are taken after full polymerization. An exact preparation protocol has been applied, which ensures reproducibility–despite the history dependence observed for actin/filamin bundle networks (18). To ensure a linear response, only small torques ($\approx$0.5 μNm) are applied. Because the effect of filamin on the linear viscoelastic moduli is extremely small, all series of experiments, in which the filamin concentration is varied at a fixed actin concentration, were conducted with one actin preparation each. This guarantees low error bars for the viscoelastic moduli ($\approx$30%) and allows for an accurate investigation of the effect of filamin on the network properties. However, the comparability of absolute values between different R-series is limited, since different actin preparations had to be used. For the viscoelastic moduli of pure actin solutions, this can result in an error of up to a factor of two—which normally is negligible, as the effect of most cross-linking molecules on the linear moduli is much more pronounced (13,22,24). To investigate the network structures, actin was labeled with phalloidin-TRITC (Sigma-Aldrich, Germany). Confocal images are taken with a confocal microscope (TCS SP5; Leica, Wetzlar, Germany). Bright-field microscopy is used to determine the distribution of bundle thicknesses in actin/filamin networks. A Gaussian is fitted to the minima in the intensity profiles perpendicular to the bundles to determine the bundle thicknesses. This method might overestimate the absolute values of the bundle diameters and might also neglect thin bundles, which are not detectable using bright-field microscopy. Nevertheless, relative changes in the distribution of bundle thicknesses are resolvable. For actin/filamin bundle clusters, a polygon approximation is applied to determine the characteristic cluster size $R = \sqrt{A}$, where A denotes the area of the polygon. Upon subtraction of the background fluorescence, the integrated fluorescence intensity of a bundle cluster is proportional to the amount of actin filaments in the cluster and can thus be used to represent the cluster mass, M (17).

RESULTS AND DISCUSSION

Structure of actin/filamin networks

Using confocal microscopy, the structure of actin/filamin networks is studied as a function of both the actin concentration c_a and the relative concentration of the ABP filamin, $R_{fil} = c_{fil}/c_a$. The actin concentration is varied from c_a = 0.95 μM up to c_a = 24 μM. The molar ratio of filamin is varied from R_{fil} = 0.001 to R_{fil} = 1. Depending on c_a and R_{fil}, different network structures are observed (Fig. 1): At low R_{fil}, the network consists of single filaments that are assumed to be cross-linked (19). Above a critical ratio R^*_{fil}, filamin induces the formation of bundles. This critical filamin ratio decreases with increasing actin concentrations (see Fig. 3). At high filamin concentrations, highly static and purely bundled actin/filamin networks are formed. There, no single filaments are detectable using confocal microscopy. In addition, microrheological experiments indicate that the number of unbundled filaments in the background of the network is very low and can be neglected. Although a high number of PEG-coated polystyrene beads of 940 nm size is observed to stick to the bundles, many others show very effective and long-ranged diffusion, which makes a tracking of the beads impossible—even for relatively short time intervals such as 50 s. For all actin concentrations investigated here, the purely bundled actin/filamin networks exhibit a common

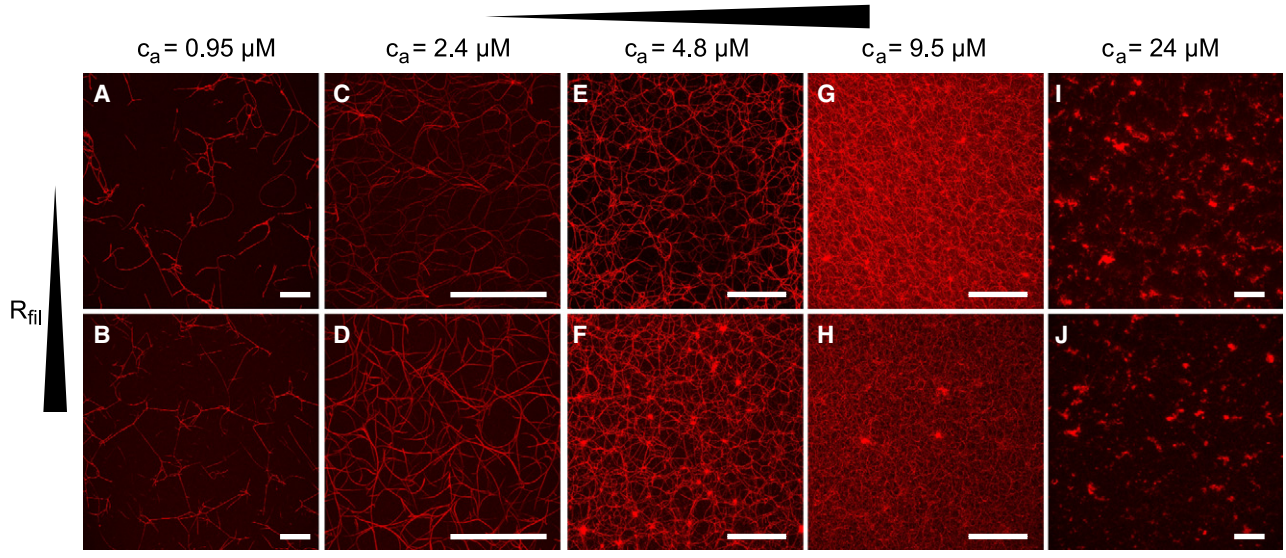

FIGURE 1 Confocal images (*A* and *B*, projections of image stacks of 120-μm height; *C* and *D*, of 60-μm height; *E–J*, of 100-μm height) of actin/filamin networks are shown for different actin concentrations and molar ratios of filamin. (*A*) c_a = 0.95 μM, R_{fil} = 0.3; (*B*) c_a = 0.95 μM, R_{fil} = 1; (*C*) c_a = 2.4 μM, R_{fil} = 0.1; (*D*) c_a = 2.4 μM, R_{fil} = 1; (*E*) c_a = 4.8 μM, R_{fil} = 0.1; (*F*) c_a = 4.8 μM, R_{fil} = 0.4; (*G*) c_a = 9.5 μM, R_{fil} = 0.03; (*H*) c_a = 9.5 μM, R_{fil} = 0.3; (*I*) c_a = 24 μM, R_{fil} = 0.02; and (*J*) c_a = 24 μM, R_{fil} = 0.1. Scale bars denote 100 μm.

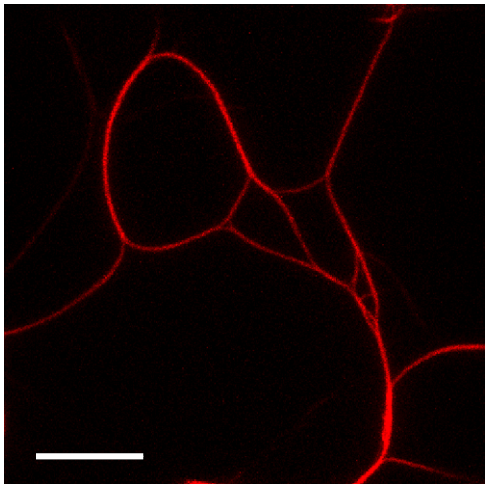

FIGURE 2 Confocal image (projection of an image stack of 20 μm height) of an actin/filamin network ($c_a = 2.4$ μM, $R_{fil} = 0.1$). Obviously, bundles are interconnected by merged bundle segments. The scale bar denotes 10 μm.

structural feature: Highly curved bundles branch and merge (Fig. 2). On the other hand, putative point-to-point cross links between distinct bundles are hardly observable (12). Moreover, because of the branched network structure, free bundle ends seem to be absent in these networks. At high actin concentrations, filamin furthermore induces the formation of bundle clusters (Fig. 1, *F–J*), which resemble the mesoscopic star-shaped heterogeneities that have been observed in actin/α-actinin networks (17).

As significant regions of the phase space of actin/filamin networks have been investigated, the observed network microstructures can be summarized in a schematic structural state diagram as a function of R_{fil} and c_a (Fig. 3).

Increasing the filamin concentration can induce drastic changes in the network architecture. However, within the purely bundled phase, a critical $R^{\#}_{fil}$ exists, above which a further increase of the filamin concentration has a surprisingly small effect on the network microstructure: The microstructures of the networks shown Fig. 1, *B*, *D*, *H*, and *J*, are virtually identical to those shown in Fig. 1, *A*, *C*, *G*, and *I*, respectively. In addition, the networks shown in Fig. 1, *E* and *F* (c_a 4.8 μM), are very similar—only that a small number of clusters is formed at $R_{fil} = 0.4$. Thus it seems that in the bundle regime the actin concentration has a stronger influence on the network structure than the filamin concentration.

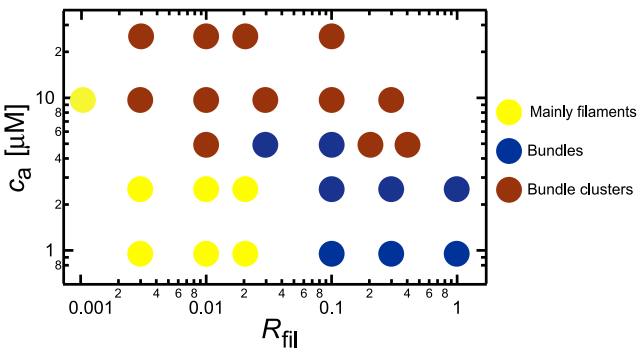

FIGURE 3 The structure of actin/filamin networks is shown as a function of the actin concentration and the molar ratio of filamin. Filamin cross-links actin filaments at low R_{fil} (*yellow*). A purely bundled network is formed at higher R_{fil} (*blue*). At high actin concentrations, bundle clusters are formed (*red*).

To quantitatively verify the observed insensitivity of the network structure toward high filamin concentrations, suitable parameters are needed to characterize the network architecture in detail. At low actin concentrations, the bundle thickness is experimentally accessible using bright-field microscopy. At high actin concentrations, however, the bundle cluster sizes can be used as a characteristic quantity.

The distribution of bundle thicknesses is determined for the actin/filamin networks shown in Fig. 1, *B–D*. A variation of the actin concentration ($c_a = 0.95$ μM and $c_a = 2.4$ μM) at a given $R_{fil} = 1$ results in different probability distributions of bundle diameters (Fig. 4 *A*): At the lower actin concentration, a significantly smaller average bundle diameter is

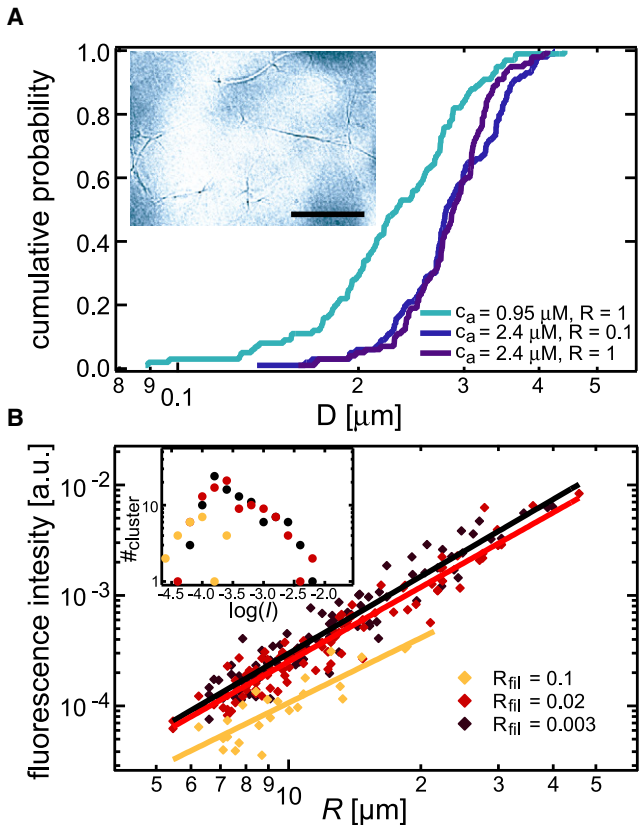

FIGURE 4 (*A*) Cumulative probabilities of bundle diameters in actin/filamin bundle networks as denoted in the legend. The inset shows an actin/filamin network ($c_a = 2.4$ μM, $R_{fil} = 1$) observed with bright-field microscopy. The scale bar denotes 20 μm. (*B*) The integrated fluorescence intensity I of bundle clusters in actin/filamin networks ($c_a = 24$ μM, R_{fil} as denoted in the legend) is plotted as a function of the characteristic cluster size, R. Lines are respective power law fits. The inset shows the corresponding distributions of cluster intensities.

observed. Yet, the bundle thickness distribution is independent of R_{fil} for a fixed $c_a = 2.4\ \mu M$ (Fig. 4 *A*). Thus, for a given c_a the actin/filamin bundle thickness is constant for high filamin concentrations. The thickness of actin bundles formed by fascin has been shown to be both limited and well defined by geometric constraints imposed by the helical structure of actin filaments (29). However, it seems improbable that such intrinsic bundle properties are responsible for the limited size of actin/filamin bundles. Because of the branched network structure, the diameters of actin/filamin bundles are broadly distributed, which is in contrast to the actin bundles formed by fascin. For actin/filamin networks, the observed structural saturation might be the consequence of the aggregation-controlled growth process, which drives the formation of the kinetically trapped actin/filamin bundle networks (18).

A diffusion-limited aggregation process has been shown to induce bundle clusters in actin/α-actinin networks (17). To allow for a comparison with this system, the actin/filamin bundle clusters occurring at high actin concentrations $c_a = 24\ \mu M$ are analyzed by determining the fluorescence intensity of the clusters. This is a suitable measure for the cluster mass and can be related to the characteristic cluster size, R, as $M \sim R^d$ (Fig. 4 *B*). For the networks shown in Fig. 1, *I* and *J*, nearly identical relations are obtained. A fractal dimension $d \approx 2.3 \pm 0.1$ is obtained from a fit to the experimental data. This value is significantly higher than the exponent $d = 1.8$ observed for actin/α-actinin networks (17). Considering that the actin/filamin clusters seem to be much denser packed, this result is very reasonable. Interestingly, the clusters formed by filamin are much larger than those observed in actin/α-actinin networks. However, the cluster properties are rather insensitive toward R_{fil} at high filamin concentrations. Not only the fractal dimension of the clusters but also the cluster mass distribution is undistinguishable for $R_{fil} = 0.02$ and $R_{fil} = 0.1$ (*inset* of Fig. 4 *B*). In contrast, a clearly different distribution is obtained for the low $R_{fil} = 0.003$. There, far fewer and smaller clusters are observed, which are also more loosely packed (Fig. 4 *B*). (Note that the increase of the cluster density with increasing filamin concentration is not a general trend. For $c_a = 9.5\ \mu M$, a high number of clusters is observed at low filamin concentrations—$R_{fil} = 0.003$ and $R_{fil} = 0.01$—but the number of clusters is clearly lower for higher ratios $R_{fil} \geq 0.03$.) Similar to the bundle thickness distribution discussed before, the analysis of the clusters confirms that the network architecture saturates at high filamin concentrations.

Considering the out-of-equilibrium character of actin/filamin bundle networks, an insensitivity of structural network parameters toward increasing filamin concentrations seems reasonable—but is nevertheless surprising: Although the resulting network structure may in general depend on R_{fil}, there is always a concentration regime, where the microstructure is almost independent of R_{fil}. Nevertheless, the addition of filamin may still change the properties of the individual bundles.

So far it has been demonstrated that depending on the actin concentration as well as the molar ratio of filamin, strongly different network architectures can be obtained: At low concentrations, filamin cross-links filamentous actin. At high filamin concentrations, bundle networks or even bundle cluster networks are formed, which show a structural saturation with respect to R_{fil}. It remains to be shown how these pronounced differences in the network structure manifest themselves in the viscoelastic network response. In the following section of this article, this question is addressed and the macromechanical response of actin/filamin networks is determined using macrorheology.

Viscoelastic response of actin/filamin networks

To characterize their linear viscoelastic properties, actin/filamin networks are first probed in the limit of small deformations. Several series of experiments with increasing filamin concentrations are conducted to study the influence of filamin on the viscoelastic response of actin/filamin networks within this linear regime. All actin concentrations used here are higher than the overlap concentration of actin filaments, which can be calculated to be $\approx 2.5\ \mu M$ (30). As an example, the obtained viscoelastic frequency spectra $G'(f)$ and $G''(f)$ of actin/filamin networks with $c_a = 9.5\ \mu M$

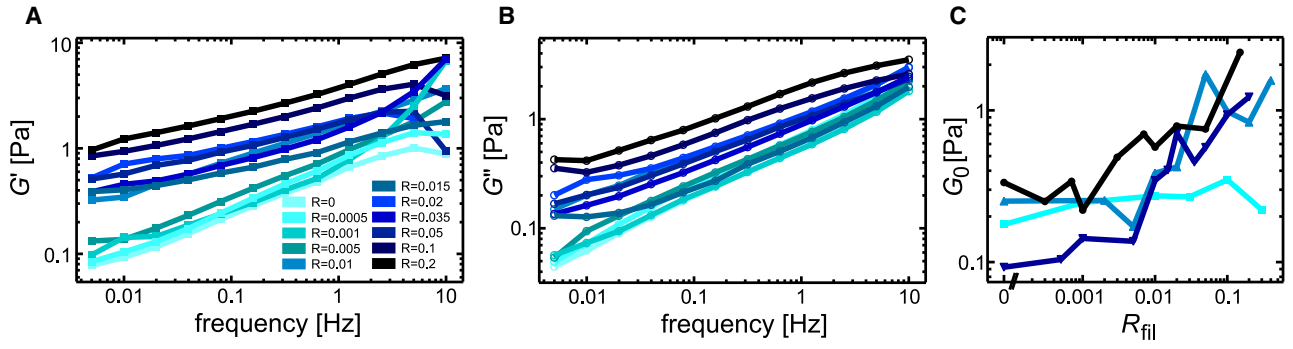

FIGURE 5 Elastic modulus $G'(f)$ (*A*) and viscous modulus $G''(f)$ (*B*) of actin/filamin networks ($c_a = 9.5\ \mu M$) are shown for different molar ratios of filamin. The color code depicted in panel *A* is also valid for panel *B*. (*C*) The apparent plateau modulus $G_0 = G'$ (10 mHz) is shown as a function of R_{fil} at different actin concentrations (*squares*, $c_a = 3.6\ \mu M$; *upright triangles*, $c_a = 4.8\ \mu M$; *inverted triangles*, $c_a = 9.5\ \mu M$; and *circles*, $c_a = 24\ \mu M$).

and varying filamin concentrations R_{fil} are depicted in Fig. 5, *A* and *B*. In contrast to actin networks cross-linked by other ABPs like HMM (31) or fascin (32), these frequency spectra are quite featureless. This indicates that in the linear network response of actin/filamin networks, there is no intrinsic timescale—at least within the experimentally accessible frequency range. To characterize the network stiffness as a function of c_a and R_{fil}, an apparent plateau modulus $G_0 := G'(10\ \text{mHz})$ is defined.

As shown in (Fig. 5 *C*), filamin significantly enhances the stiffness of actin networks for $c_a > 3.6\ \mu M$. However, the effect of filamin on the linear stiffness of the actin network is rather weak compared to other actin cross-linking molecules like HMM (22), fascin (24), scruin (13), or α-actinin (33). For all actin concentrations investigated here, even the addition of high filamin concentrations enhances the apparent plateau modulus G_0 by less than one order of magnitude. At least for the filamentous networks this can be rationalized considering the high flexibility of individual filamin molecules (21). For the bundled networks, the weak increase in the linear network stiffness is rather surprising—especially since actin/filamin bundle networks exhibit internal stresses (18), which would be expected to enhance the network elasticity (21,34).

So far we have studied the viscoelastic properties of actin/filamin networks exclusively in the limit of small deformations, i.e., in the linear regime. There, the influence of filamin on the network elasticity is rather small—but not its influence on the network structure. As a consequence, a precise correlation of structural and mechanical network properties is highly difficult. Thus, we now address the nonlinear network properties at high deformations, where the effect of filamin has been reported to be much stronger (21). This nonlinear regime is investigated best with a constant shear rate $\dot{\gamma}$ to minimize creep artifacts during the measurement. A shear rate $\dot{\gamma} = 20\%\ s^{-1}$ is used for $c_a = 4.8\ \mu M$, and $\dot{\gamma} = 12.5\%\ s^{-1}$ is used for all other actin concentrations. From the recorded stress-strain relation $\sigma(\gamma)$ the differential modulus $K(\gamma) = \frac{\partial \sigma}{\partial \gamma}$ is calculated (35).

Fig. 6 *A* shows the nonlinear response for actin/filamin networks with $c_a = 9.5\ \mu M$ and varying filamin concentrations. The addition of filamin clearly enhances the strain-hardening behavior of actin networks. The dependence of the maximal nonlinear network stiffness K_{max} and the corresponding yield stress σ_{max} on R_{fil} is similar for all actin concentrations investigated here (Fig. 6, *B* and *C*): At low molar ratios of filamin, both parameters increase strongly. This trend continues up to filamin concentrations that roughly correspond to the regime where bundle networks are formed. Note that for low actin concentrations ($c_a = 3.6\ \mu M$ and $c_a = 4.8\ \mu M$), pure actin solutions do not show strain-hardening at the experimental conditions used here—but filamin induces strain-hardening for $R_{fil} \geq 0.01$. At high R_{fil}, an insensitivity of σ_{max} and K_{max} toward the filamin concentration is observed. We speculate that the saturation of σ_{max} and K_{max} in the bundle regime is directly correlated with the observed insensitivity of the structural network properties with respect to high filamin concentrations. Although the network architecture saturates at high R_{fil}, an increased filamin concentration may still change the interconnectivity of distinct bundles, which is generated by cross links formed by filamin, as well as the degree of cross-linking between individual actin filaments within a bundle. This might not only explain the fact that the apparent plateau modulus G_0 is still increasing, but also the observation that the shape of the nonlinear response $K(\gamma)$ becomes broader with increasing R_{fil}.

It has been shown before that the interconnectivity of actin networks, i.e., the presence of transient cross links, gives rise to a pronounced loading rate dependence of the nonlinear response, which is based on forced unbinding events of distinct cross links (34). Thus, we perform shear-rate-dependent measurements to address the influence of the filament/filament or bundle/bundle interconnectivity on the nonlinear response of actin/filamin networks. Indeed, the nonlinear response of actin/filamin bundle networks ($c_a = 4.8\ \mu M$) strongly depends on the shear rate $\dot{\gamma}$ (Fig. 7): With decreasing shear rates the maximum nonlinear stiffness K_{max} decreases

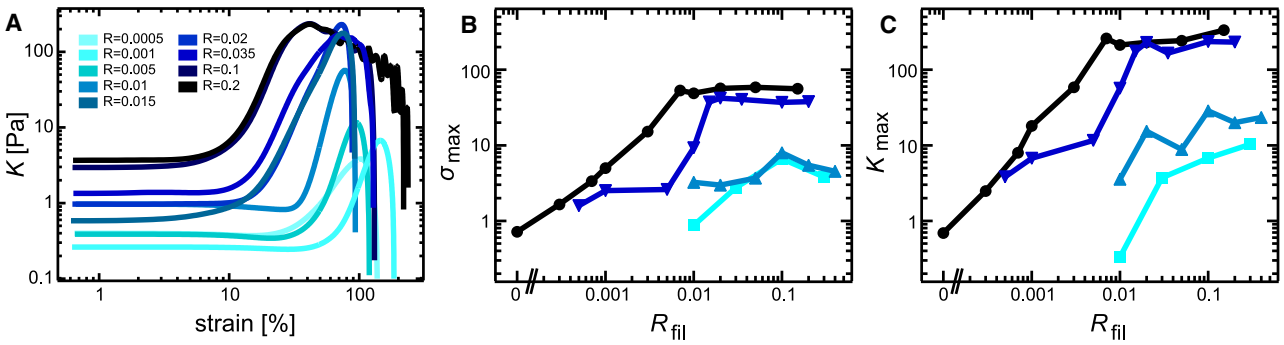

FIGURE 6 (*A*) The differential modulus *K* is shown as a function of strain for different molar ratios of filamin ($c_a = 9.5\ \mu M$). The values σ_{max} (*B*) and K_{max} (*C*) are plotted as a function of R_{fil} for different actin concentrations (*squares*, $c_a = 3.6\ \mu M$; *upright triangles*, $c_a = 4.8\ \mu M$; *inverted triangles*, $c_a = 9.5\ \mu M$; and *circles*, $c_a = 24\ \mu M$).

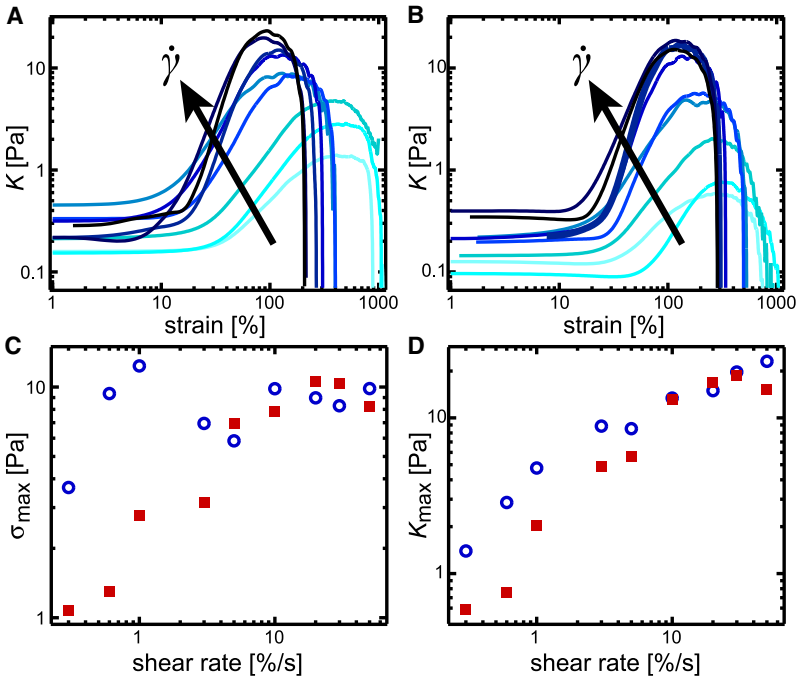

FIGURE 7 The differential modulus K of actin/filamin bundle networks ($c_a = 4.8\ \mu$M) (A) $R_{fil} = 0.072$; (B) $R_{fil} = 0.216$ is shown as a function of strain for different shear rates. The corresponding σ_{max} (C) and K_{max} (D) are plotted as functions of $\dot{\gamma}$. The values $R_{fil} = 0.072$ and $R_{fil} = 0.216$ are denoted as circles and squares, respectively.

by more than one order of magnitude; in addition, σ_{max} decreases toward low shear rates. Moreover, for low shear rates, K_{max} is reached at higher strains—a reorganization of the actin/filamin network during the shear experiment might be possible because of unbinding events of transient actin/filamin cross links giving rise to a flow behavior of the network. The independence of σ_{max} and K_{max} of R_{fil} in the purely bundled regime (Fig. 6 C) holds true only for shear rates $\dot{\gamma} \gtrsim 10\%\ s^{-1}$. At low shear rates, both parameters depend on the filamin concentration (Fig. 7, C and D). Although increasing filamin concentrations induce no additional structural changes, they suffice to alter the mechanical properties—most probably by increasing the interconnectivity, i.e., the cross-link density between merged bundle segments or between actin filaments in the bundles. The observed dependence on R_{fil} suggests that for high shear rates the nonlinear response is dominated by the network structure. At low $\dot{\gamma}$, however, the interconnectivity—which depends on the filamin concentration—plays a more important role, as σ_{max} and K_{max} depend on R_{fil}. It can be speculated that the critical shear rate $\dot{\gamma} = 10\%\ s^{-1}$, below which σ_{max} and K_{max} depend on R_{fil}, corresponds to the timescale necessary for sufficient unbinding and rebinding events of filamin molecules to allow for structural reorganizations during the shear experiment.

CONCLUSION

In conclusion, we have shown that actin/filamin networks exhibit various network architectures which depend on the concentration of both proteins. In addition to cross-linked filamentous networks, bundle networks are observed as well as highly heterogeneous bundle cluster networks. A structural saturation occurs at high filamin concentrations although not all binding sites are occupied. This structural insensitivity toward the molar ratio of filamin manifests itself also in the nonlinear viscoelastic network properties. Although the transition from a regime of cross-linked filaments to a purely bundled regime is accompanied by a strong increase of the maximal nonlinear stiffness K_{max} and the corresponding yield stress σ_{max}, both parameters are constant at higher filamin concentrations. At these high filamin concentrations, the structure of actin/filamin networks is determined by an aggregation-controlled growth process (18) rather than by thermal equilibrium. This may account for the observed structural insensitivity with respect to the filamin concentration. However, the linear network stiffness G_0 still increases as a function of R_{fil}—which is most probably due to an increasing bundle stiffness. Our results demonstrate that actin/filamin networks exhibit various network structures which entail distinct linear and nonlinear viscoelastic properties. Therefore, theoretical descriptions of the mechanical properties of actin/filamin networks must take into account these different network structures. The detailed characterization of actin/filamin networks presented here sets the basis for further studies addressing the microscopic origin of the structural transitions in living cells as well as their consequences on the macromechanical properties of the cytoskeleton.

We thank M. Rusp for the actin preparation.

Financial support of the German Excellence Initiatives via the Nanoinitiative Munich (NIM), the Munich-Centre for Advanced Photonics (MAP), and by the DFG through Grant No. Ba2029/8-1 is gratefully acknowledged.

REFERENCES

1. Trepat, X., G. Lenormand, and J. J. Fredberg. 2008. Universality in cell mechanics. *Soft Matter*. 4:1750–1759.
2. Stossel, T. 1993. On the crawling of animal cells. *Science*. 260:1086–1094.
3. Bausch, A. R., and K. Kroy. 2006. A bottom-up approach to cell mechanics. *Nat. Phys*. 2:231–238.
4. Kasza, K. E., A. C. Rowat, J. Liu, T. E. Angelini, C. P. Brangwynne, et al. 2007. The cell as a material. *Curr. Opin. Cell Biol*. 19:101–107.
5. Huisman, E. M., T. van Dillen, P. R. Onck, and E. Van der Giessen. 2007. Three-dimensional cross-linked F-actin networks: relation between network architecture and mechanical behavior. *Phys. Rev. Lett*. 99:208103.
6. Conti, E., and F. C. MacKintosh. 2009. Cross-linked networks of stiff filaments exhibit negative normal stress. *Phys. Rev. Lett*. 102:088102.
7. Heussinger, C., B. Schaefer, and E. Frey. 2007. Nonaffine rubber elasticity for stiff polymer networks. *Phys. Rev. E Stat. Nonlin. Soft Matter Phys*. 76:031906.
8. Head, D. A., A. J. Levine, and F. C. MacKintosh. 2003. Deformation of cross-linked semiflexible polymer networks. *Phys. Rev. Lett*. 91: 108102.
9. Wilhelm, J., and E. Frey. 2003. Elasticity of stiff polymer networks. *Phys. Rev. Lett*. 91:108103.
10. Astroem, P., B. S. Kumar, I. Vattulainen, and M. Karttunen. 2008. Strain hardening, avalanches, and strain softening in dense cross-linked actin networks. *Phys. Rev. E Stat. Nonlin. Soft Matter Phys*. 77:051913.
11. Wagner, B., R. Tharmann, I. Haase, M. Fischer, and A. R. Bausch. 2006. Cytoskeletal polymer networks: molecular structure of cross-linkers determine macroscopic properties. *Proc. Natl. Acad. Sci. USA*. 103:13974–13978.
12. Schmoller, K. M., O. Lieleg, and A. R. Bausch. 2008. Cross-linking molecules modify composite actin networks independently. *Phys. Rev. Lett*. 101:118102.
13. Shin, J. H., M. L. Gardel, L. Mahadevan, P. Matsudaira, and D. A. Weitz. 2004. Relating microstructure to rheology of a bundled and cross-linked F-actin network in vitro. *Proc. Natl. Acad. Sci. USA*. 101:9636–9641.
14. Tseng, Y., E. Fedorov, J. M. McCaffery, S. C. Almo, and D. Wirtz. 2001. Micromechanics and ultrastructure of actin filament networks crosslinked by human fascin: a comparison with α-actinin. *J. Mol. Biol*. 310:351–366.
15. Tseng, Y., K. M. An, O. Esue, and D. Wirtz. 2004. The bimodal role of filamin in controlling the architecture and mechanics of F-actin networks. *J. Biol. Chem*. 279:1819–1826.
16. Volkmer Ward, S. M., A. Weins, M. R. Pollak, and D. A. Weitz. 2008. Dynamic viscoelasticity of actin cross-linked with wild-type and disease-causing mutant α-actinin-4. *Biophys. J*. 95:4915–4923.
17. Lieleg, O., K. M. Schmoller, C. J. Cyron, W. A. Wall, and A. R. Bausch. 2009. Structural polymorphism in heterogeneous cytoskeletal networks. *Soft Matter*. 5:1796–1803.
18. Schmoller, K. M., O. Lieleg, and A. R. Bausch. 2008. Internal stress in kinetically trapped actin bundle networks. *Soft Matter*. 4:2365–2367.
19. Stossel, T. P., J. Condeelis, L. Cooley, J. H. Hartwig, A. Noegel, et al. 2001. Filamins as integrators of cell mechanics and signaling. *Nat. Rev. Mol. Cell Biol*. 2:138–145.
20. Feng, Y., and C. A. Walsh. 2004. The many faces of filamin: a versatile molecular scaffold for cell motility and signaling. *Nat. Cell Biol*. 6: 1034–1038.
21. Gardel, M. L., F. Nakamura, J. H. Hartwig, J. C. Crocker, T. P. Stossel, et al. 2006a. Prestressed F-actin networks cross-linked by hinged filamins replicate mechanical properties of cells. *Proc. Natl. Acad. Sci. USA*. 103:1762–1767.
22. Tharmann, R., M. M. A. E. Claessens, and A. R. Bausch. 2007. Viscoelasticity of isotropically cross-linked actin networks. *Phys. Rev. Lett*. 98:088103.
23. Gardel, M. L., F. Nakamura, J. H. Hartwig, J. C. Crocker, T. P. Stossel, et al. 2006. Stress-dependent elasticity of composite actin networks as a model for cell behavior. *Phys. Rev. Lett*. 96:088102.
24. Lieleg, O., M. M. A. E. Claessens, C. Heussinger, E. Frey, and A. R. Bausch. 2007. Mechanics of bundled semiflexible polymer networks. *Phys. Rev. Lett*. 99:088102.
25. Spudich, J. A., and S. Watt. 1971. Regulation of rabbit skeletal muscle contraction. 1. Biochemical studies of interaction of tropomyosin-troponin complex with actin and proteolytic fragments of myosin. *J. Biol. Chem*. 246:4866–4871.
26. Janmey, P. A., J. Peetermans, K. S. Zaner, T. P. Stossel, and T. Tanaka. 1986. Structure and mobility of actin filaments as measured by quasielastic light scattering, viscometry, and electron microscopy. *J. Biol. Chem*. 261:8357–8362.
27. Kurokawa, H., W. Fujii, K. Ohmi, T. Sakurai, and Y. Nonomura. 1990. Simple and rapid purification of brevin. *Biochem. Biophys. Res. Commun*. 168:451–457.
28. Shizuta, Y., H. Shizuta, M. Gallo, P. Davies, and I. Pastan. 1976. Purification and properties of filamin, an actin binding protein from chicken gizzard. *J. Biol. Chem*. 251:6562–6567.
29. Claessens, M. M. A. E., C. Semmrich, L. Ramos, and A. R. Bausch. 2008. Helical twist controls the thickness of F-actin bundles. *Proc. Natl. Acad. Sci. USA*. 105:8819–8822.
30. Kroy, K., and E. Frey. 1996. Force-extension relation and plateau modulus for wormlike chains. *Phys. Rev. Lett*. 77:306–309.
31. Lieleg, O., M. M. A. E. Claessens, Y. Luan, and A. R. Bausch. 2008. Transient binding and dissipation in semi-flexible polymer networks. *Phys. Rev. Lett*. 101:108101.
32. Lieleg, O., and A. R. Bausch. 2007. Cross-linker unbinding and self-similarity in bundled cytoskeletal network. *Phys. Rev. Lett*. 99:158105.
33. Tempel, M., G. Isenberg, and E. Sackmann. 1996. Temperature-induced sol-gel transition and microgel formation in α-actinin cross-linked actin networks: a rheological study. *Phys. Rev. E Stat. Phys. Plasmas Fluids Relat. Interdiscip. Topics*. 54:1802–1810.
34. Lieleg, O., K. M. Schmoller, M. M. A. E. Claessens, and A. R. Bausch. 2008. Cytoskeletal polymer networks: viscoelastic properties are determined by the microscopic interaction potential of cross-links. *Biophys. J*. 96:4725–4732.
35. Semmrich, C., R. J. Larsen, and A. R. Bausch. 2008. Nonlinear mechanics of entangled F-actin solutions. *Soft Matter*. 4:1675–1680.